Systematic Wavelength Shifts of the MOI si425 Sensing Interrogator at Low Signal Intensities

Helmut WOSCHITZ
Graz University of Technology
Institute of Engineering Geodesy and Measurement Systems
Steyrergasse 30, A-8010 Graz, Austria

Abstract. For the investigation of the performance of elastic rail pads several FBG sensors were embedded into these very small structures (195 x 150 x 7 mm^3). The elastic pads are used in railway engineering as damping elements in between the rail and the sleeper. They are deformed during the passage of a train by 3 % in the horizontal direction and 10 % in the vertical direction.

In field investigations with an embedded FBG temperature sensor, atypical signals with wavelength changes of about 5 nm within a fraction of a second were observed. But as the sensor is not able to follow such fast temperature changes, these signals must be affected. Changes of the signal intensity depending on the applied load and the pad's compression were identified as one possible error source.

For the interrogator used there is no information available about the wavelength stability in the case of varying signal intensity. Thus a laboratory experiment was carried out, where the signal intensities were artificially attenuated. Several commercially available FBG sensors of different manufacturers were used in the experiment.

The wavelengths were found to be unaffected over a rather wide dynamic range. However, at very low signal intensities, systematic wavelength shifts of up to 20 pm were observed. These are correlated to the signal intensity and thus it is possible to model them and to correct affected data.

1. Introduction

Knowledge about the precision of a measurement system is essential in order to be able to plan individual measuring tasks (e.g. choosing the appropriate instrument, sampling rate, …). Especially, for the derivation of measurement uncertainty this knowledge is crucial. But for fiber optic systems there is often only little information available aside the one given by the manufacturer (e.g. in the specifications). Thus, it may be difficult to assess the capabilities of an instrument, the more, as manufacturers sometimes use a different terminology in their specifications.

Since 2004 we own a Micron Optics si425 interrogator for the reading of Fiber-Bragg-Gratings. The manufacturer provides a detailed document about the testing performance of this instrument (Micron Optics, 2003). But aside this, there are almost no reports in the literature about independent testing or practical experiences with this instrument.

Licence: http://creativecommons.org/licenses/by-nd/3.0

However, it is interesting to know whether or not low signal intensities have an influence on the measured wavelength, at least for some very specific measuring tasks. Of course, the gain value of the instrument should be set properly prior to the measurement, but what happens if the signal intensity varies as a result of bending effects of the lead in fiber? This might get a critical issue, especially if the signal intensity is rather low, e.g. when using FBGs with a low reflectance.

Such gratings offer a higher mechanical strength compared to standard gratings and therefore had to be used for the investigation of elastic rail pads due to the large strains inside the pad which emerge when the load of a train is applied. When using FBG based sensors to measure the temperature inside the pad, atypical signals were found for one sensor, see chapter 2. Thus, an experiment in our laboratory was planned in order to investigate this effect. The hardware used within this experiment is briefly described in chapter 3, and its realisation is summarized in chapter 4. Results of the experiment are shown in chapter 5, where the dependence of the wavelengths on signal intensities is studied too. Based on these results, a calibration function is derived in order to correct affected measurements. Finally, the results and their importance for practical field measurements are discussed in chapter 6.

2. Motivation: An experience from a field experiment

In railway engineering elastic pads are used in between the rail and the sleeper in order to reduce the stress in the roadbed and track components. In Austria, these pads often need to be replaced after very short time spans (every 2.5 to 4 years, Auer, 2005), especially in alpine regions. The reason for the short life time of the pads is rather unknown. Thus, investigations should be performed with strain measurements inside the elastic pad during the passage of trains. As the pads are rather small (e.g. 195 x 150 x 7 mm^3), fiber optic sensors appeared to be the only suitable sensor type. The material used for the pads is a closed-cell polyurethane elastomer (PU) with a rather low static stiffness (about 160 kN/mm). Several FBG sensors were embedded into the pad whilst manufacturing (for details see Woschitz, 2010). Most sensors were used as strain sensors in order to determine the strain distribution inside the pad during the passage of a train. Using these sensing pads, nonlinear strain behaviour in the interior of the pads was discovered for the first time, Woschitz (2011).

Additionally, one elastic pad was instrumented with three FBG based temperature sensors (FBG-t°) to study its temperature distribution. The FBG sensors were cut a few millimetres after the grating and glued into a small steel tube in order to protect the grating from strain and pressure, see fig. 1. A bare fiber was attached to the other end of the tube which allows tensioning the fiber sensor whilst manufacturing the pad. This was necessary for the proper positioning of FBG-t° sensor in the middle of the pad. Commercially available sensors were not appropriate for this task.

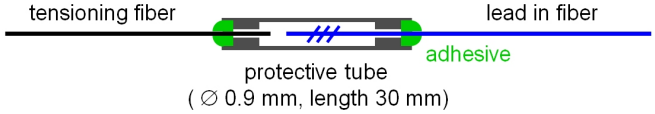

Figure 1. Schema of the used FBG-based temperature sensor

Fig. 2a schematically shows the layout of the sensing pad, the positions of the FBG-t° sensors and their lead in fibers, whereas fig. 2b shows the pad's position in between the rail and the sleeper.

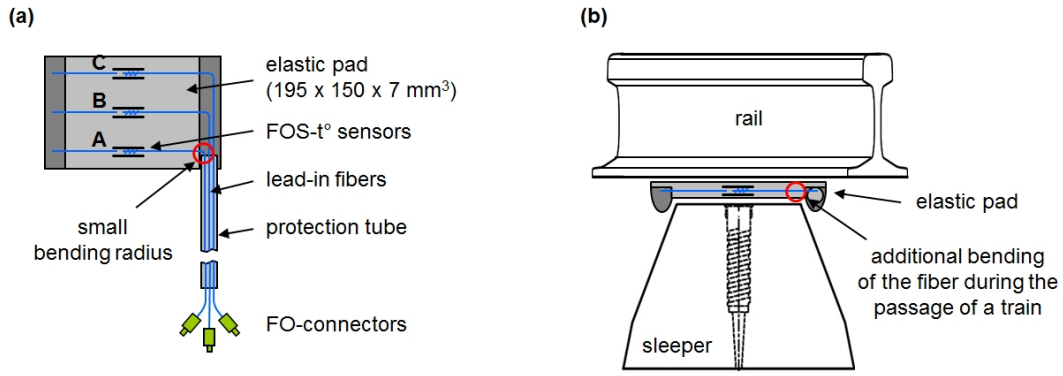

Figure 2. Schema of the FBG-t° sensors inside the elastic rail pad, (a) ground view and (b) plan view of the pad between the rail and the sleeper

The temperature sensing pad was used during a field experiment on a real railway track. There, the temperature increase caused by the compression of the pad (~ 10 %) during the passage of a train should be measured, as this was unknown for the material used. Exemplarily, the raw and filtered temperature data of sensor A (see fig. 2a) that were acquired during the passage of a cargo train (71 axis) are shown in fig. 3. The sampling frequency was 250 Hz and the wavelength resolution was 1 pm.

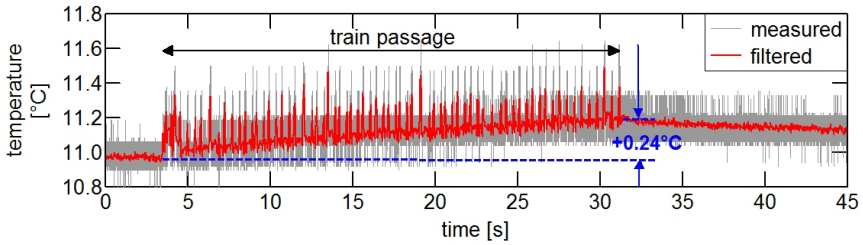

Figure 3. Temperature inside an elastic pad during the passage of a train, measured with an FBG based temperature sensor

Caused by the compression of the pad, the temperature gradually increases by 0.24 K during the passage of the train. Afterwards, the temperature slowly decreases again because of heat dissipation. However, each time an axis of the train is above the sensing pad, the signal shows a sudden increase in temperature (approx. 0.4 K within a time period of < 0.1 s). But it is known from calibration that the FBG-t° sensors used are not able to follow such fast temperature changes (their time constant is $\tau \sim 0.5$ s). Furthermore, it is known from testing the pad that the FBG-t° sensors are insensitive to accelerations. Additionally, sensors B and C do not show these sudden temperature increases. Therefore, a sensor effect can be excluded as a possible reason for these atypical temperature signals. However, during the passage of the train the part of the pad which touches both, the rail and the sleeper, is compressed by about 10 %, whilst the remaining parts are not. This causes an additional bending of the lead in fiber (fig. 2b) which cannot be avoided due to constructive reasons of the elastic pads. Thus, signal disturbances caused by these bending effects are considered as a possible reason for this atypical behaviour of the sensor which will be further investigated in this paper.

3. Measurement equipment used

3.1 Micron Optics si425 sensing interrogator

For the following experiments, a MOI si425-200 V1.1 sensing interrogator (version 1.19) was used. Its main specifications are listed in tab. 1.

Table 1. Main specifications of the MOI si425 sensing interrogator (Micron Optics, 2004 and 2006)

– measurement range:	1520 - 1570 nm
– optical resolution:	1 pm
– wavelength stability:	2 pm typ. (5 pm max., over time and temperature range)
– wavelength repeatability:	0.5 pm at full speed, 0.05 pm with 250 averages
– dynamic range:	15 dB
– maximum sampling frequency:	250 Hz
– number of optical channels:	4
– max. number of sensors per channel:	32
– maximum distance to sensor:	> 50 km
– heating-up time:	5 min
– operating temperature:	+10°C to +40°C
– calibration:	never needed (wavelength is calibrated on every scan)

The measurement technology of the interrogation unit is based on a swept laser and the wavelength of a sensor is basically derived by measuring the time of flight. Peak detection is implemented in the hardware of the interrogator and the wavelengths of the detected sensors are sent to a host computer where they can be stored using a LabView based software. Peak detection is implemented in the interrogator and details about the used peak detection algorithm are not known to the common user. Information about the full spectrum is not applicable when using this instrument.

For weak signals the gain of the instrument can be increased which is generally done prior to data acquisition. As a criterion for the proper setting of the gain, a measure of the signal intensity (i.e. the ″level″, dimensionless units, $0 < \text{level} < 255$) is output. The level of the signal should be between two limits, which are graphically given only but might be approx. about 10 and 225.

Signals with the level above 225 might saturate the photo detectors and by this the detected wavelengths can get significantly wrong (Micron Optics, 2004, p.12). Signals below a level of 10 might give results that ″may not be optimal″ (Micron Optics, 2004, p.12). However, a more detailed statement like a maximum deviation from the unaffected wavelength is not given. But under the view of measurement uncertainty such information is necessary, especially for cases where the signal intensity changes during the measurement. Thus for the investigations described later in this paper, the standard software was modified in order to store the signal levels too.

3.2 FBG sensors used

For the interrogator used, there is no recommendation for a specific type of FBG sensor to be used. The only brief statement regards to the uses of apodized gratings (Micron Optics, 2004, p. 65). However, several manufacturers of FBGs or FBG based sensors do not even give such details about their gratings or their sensors respectively. Thus, for testing purposes 9 FBG sensors of different manufacturers were used, which were purchased within the last few years. Their wavelengths are spread across the whole measuring range of the interrogator and they have a rather high reflectivity in order to get high signal levels

(about 160 which is well below the upper limit of saturation). Their specifications are listed in tab. 2.

Table 2. Available details about the FBG sensors used

sensor no.	λ_c [1] [nm]	BW [2] [nm]	grating length [mm]	reflectivity [%]	coating	core diameter [μm]	manufacturer
1	1523.850	0.145	5	17.0	Ormocer	4 [3]	FBGS Intl. (DTG)
2	1530.228	0.514	5	85.0	Acrylat	9	Welltech
3	1532.0* [4]	*	* [4]	*	Polyimide	9	Avensys
4	1540.088	0.151	15	87.3	Polyimide	9	FBGS Intl.
5	1542.0*	*	*	*	Polyimide	9	Avensys
6	1544.937	0.501	5	83.9	Acrylat	9	Welltech
7	1552.0*	*	*	*	Polyimide	9	Avensys
8	1555.154	0.225	15	94.4	Polyimide	9	FBGS Intl.
9	1559.989	0.490	5	80.3	Acrylat	9	Welltech
10	1562.0*	*	*	*	Polyimide	9	Avensys

[1] Central wavelength, [2] bandwidth (3dB), [3] Draw Tower Grating, [4] not applicable (*)

Grating no. 1 is a Draw Tower Grating with excellent mechanical performance. However, the reflectivity of the FBG is the lowest of the used gratings. All other gratings were manufactured with the recoating process. None of the gratings was used before, thus all of them were in a pristine state.

The gratings were spliced together in order to create a FBG chain (total length about 25 m) which makes it easy to measure all gratings simultaneously, using one channel of the interrogator only.

4. Description of the experiment

4.1 Setup

The performance of the interrogator's wavelength detection at very low signal levels should be determined in the experiment. Thus, the FBG sensors should be unaffected of strain or temperature changes during the whole experiment. Assuming a standard thermo optic coefficient of approx. 10 pm/K for the sensors and a repeatability of 0.05 pm for the measurement (see tab. 1), a very high temperature stability of < 0.01 K is needed. In order to be able to achieve this, the 25 m long sensor chain was wound up with a diameter of about 10 cm and afterwards this fiber roll was put into small a box. Winding does not affect the experiment as was investigated separately, but will not be shown here.

The box was put at the bottom of a 2 m deep shaft in our laboratory, because there are almost no temperature changes over several hours. The experiments were started after sufficiently acclimatisation time. The temperature in the shaft was independently controlled by measurements of a PT100 sensor and remained stable within its measurement precision (< 0.02 K).

4.2 Modification of the signal intensity

The signal was attenuated by (a) macrobending of the lead in fiber or (b) by an air gap of variable width, interrupting the lead in fiber. Anyway, both methods yield rather the same result.

4.3 Data pre-processing

Data were acquired with 250 Hz. Afterwards the data of consecutive sections, each of 25 samples, were averaged in order to reduce noise.

5. Results

5.1 Wavelength shifts

In chapter 2 it was assumed that there is a dependency of the measured wavelength on the signal intensity which now should be experimentally verified in the laboratory. For the shown data, signal attenuation was done using an air-gap in order to drop down the signal intensities to a very small level, even down to zero, where the sensors could not be detected any more.

Fig. 4 shows the results for all sensors listed in tab. 2. In order to allow better comparison, the wavelengths were reduced for their initial values, fig. 4a. The corresponding signal intensities are shown in fig. 4b.

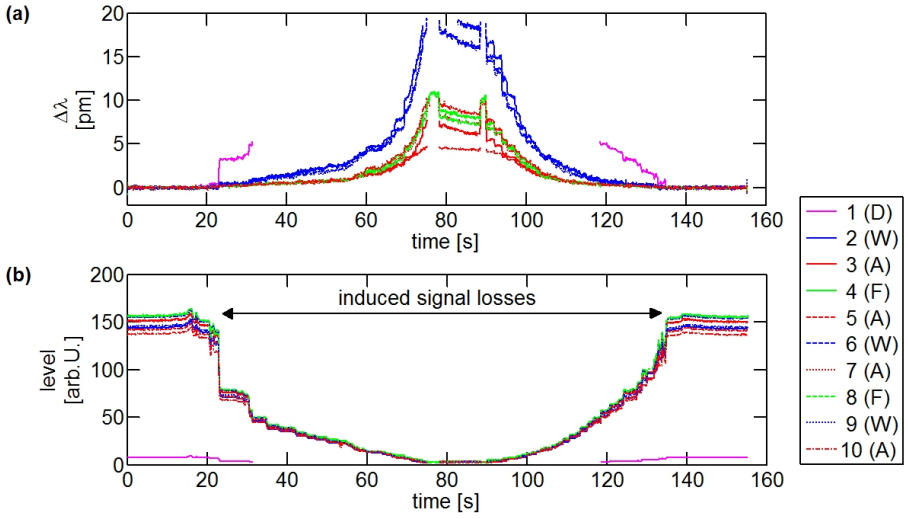

Figure 4. (a) Wavelength shifts (Δλ) caused by signal attenuation and (b) corresponding signal intensities (levels)

Signal attenuation starts approx. at 18 s and by this the levels start to decrease. First wavelength shifts can be seen for sensor #1 (pink in fig. 4) and these shifts get up to 6 pm, before the signal of the sensor is lost (at 32 s). However, this sensor already had low signal intensity (level < 10) at the beginning because of the low reflectance of the grating and due to splice losses (smaller core diameter, see tab. 2). Thus, the results of this sensor will not be used in the following discussions. The other sensors have much higher signal intensities at the beginning (levels about 150) and therefore wavelengths shifts increase to a significant level. In the section of very low signal intensities (levels below 10; approx. from 65 s to 100 s) maximum shifts of about 20 pm can be observed for sensors #2, 6 and 9. Although, there are also differences between the sensors of the same manufacturer, there is a certain systematic for the sensors of the same type. However, there is not sufficient information available (see tab. 2) for the sensors which would allow a deeper study on this subject. Afterwards, with increasing signal intensities, the wavelengths get back to their initial value.

5.2 Wavelength shifts vs. signal intensities

In the next step, the observed wavelength shifts are compared to their corresponding signal intensities, fig. 5.

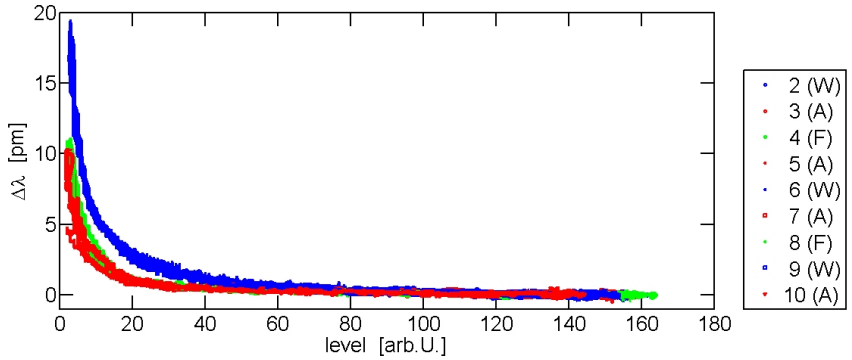

Figure 5. Wavelength shifts (Δλ) vs. signal intensities (level)

Here, the systematic behaviour of the different sensor types can be seen more clearly. The wavelengths detected with the MOI si425 in combination with the FBGS and Avensys sensors shift about half of the magnitude compared to those with the Welltech sensors.

At the critical level of 10, the wavelengths shifts are about 6 pm at maximum, which is a more detailed information than the one given by the manufacturer (see section 3.1).

5.3 Calibration function

During other investigations at our institute it was found, that a combination of two exponential functions of different shape models the data best (Moser, 2011):

$$\Delta\lambda = a \cdot e^{b \cdot L} + c \cdot e^{d \cdot L} \tag{1}$$

There, L is the measured level and the unknown parameters are a to d. For parameter estimation of this nonlinear calibration function, good approximate values are needed for the least squares adjustment.

In the case that sensors of the same type have a similar behaviour, a common calibration function can be derived. For the example shown here, this was done for the three Welltech sensors (#2, 6 and 9), where the parameters were estimated as a= 29.1 pm, b= -0.31, c= 6.7 pm and d= -0.04. Both, data and the modelled calibration function are shown in fig. 6a and the corresponding residuals are depicted in fig. 6b.

The residuals are about 0.5 pm for levels > 10 and about 3 pm at the smallest level, which is mainly caused by remaining minor differences between the three sensors. Thus, in the following one individual calibration function was derived for each sensor in order to take account of these minor differences.

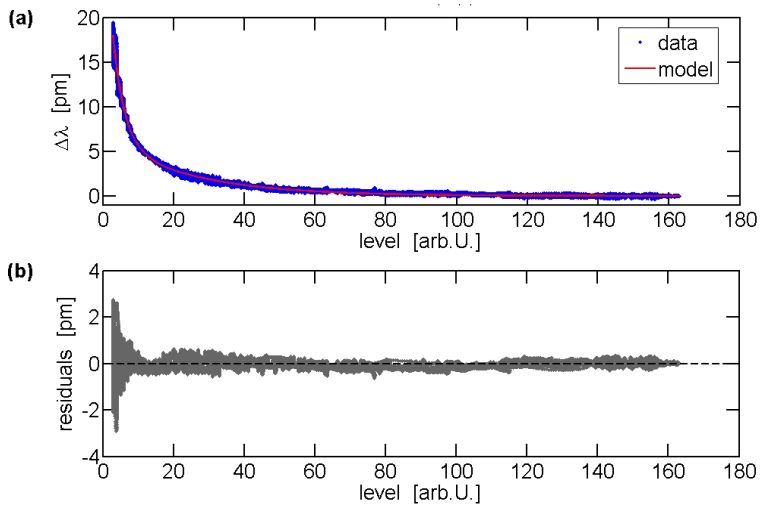

Figure 6. (a) Data with an estimated calibration function and (b) its residuals

5.6 Correction of data using the calibration function

Fig. 7a shows the data of another measurement (14 days later, same sensors, but without the low level sensor #1). In the beginning of the data set (until 18 s) and at the end (starting from 58 s) the level was about 150 for all sensors and in between, the level dropped down to 2 due to signal attenuation. By this, the signals were shifted up to 20 pm.

These data were now corrected using the individual calibration functions, see fig. 7b.

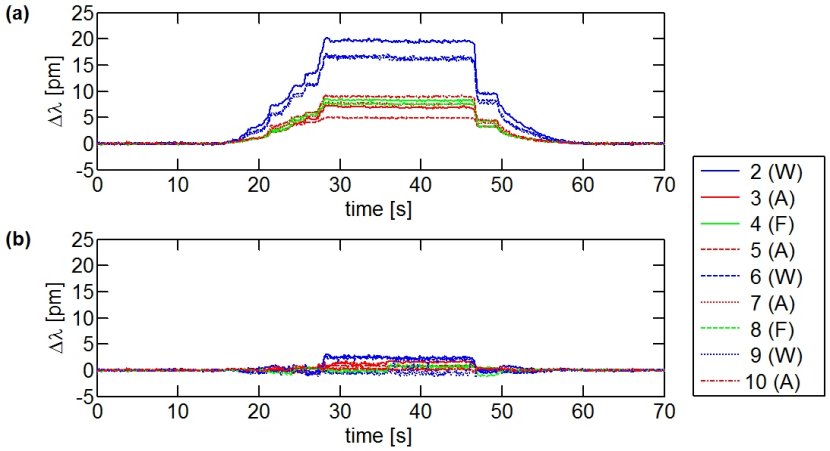

Figure 7. (a) Data of another measurement with levels close to zero in the middle section, and (b) corrected data using individual calibration functions

By this means, the signal deviations can be reduced by a factor of 7. The remaining deviations are less than 3 pm and arise in the middle section, where the signals have very low intensities that are close to zero.

6. Conclusion

For the interrogation of FBG sensors a Micron Optic si425 instrument was used. The manufacturer states that measurements at small signal levels might give results that ″may not be optimal″ (Micron Optics, 2004, p.12). The meaning of this imprecise statement was investigated by several experiments. There, systematic wavelength shifts of up to 20 pm

were observed if the signal intensity goes down to a small value. This corresponds to an error of about 15 με in a strain or about 2 K in a temperature measurement. Thus, a better understanding of this systematic effect is essential for practical measurements where high precision is needed.

The wavelength shifts were found to be correlated to the signal intensity, and thus calibration functions could be derived for the used sensors. These calibration functions can be applied to field data, if information about the signal intensity is available for them. As a result of this correction, signal shifts that appear at low levels can be reduced by a factor of 7. However, further studies on the generalisation of the calibration function will be carried out.

The interrogator used (MOI si425) can be programmed to output the signal levels that are needed for data correction continuously. However, signal levels are not available for all channels for the follow up instrument (MOI sm130). Thus, it is neither possible to correct data nor to assess the accuracy level of the data. But then, in the case that data are obviously affected (like the one shown in chapter 2 which were acquired using a MOI sm130), one might only state ″There's something wrong″, which – of course – is rather unsatisfying.

For standard users it is proposed, that the manufacturers modify the data acquisition software in a way that no (affected) data are output at low signal intensities. However, for enhanced users additional information like signal intensity, a quality parameter of the peak detection, the bandwidth of the signal or best the whole spectrum available during the measurement (synchronous to the wavelength data) should be accessible, at least in an expert mode. This is in my opinion one of the key issues to be able to specify measurement uncertainty and thus get reliable results, even in non-standard environments like non-linear strain, or signal disturbances by bending effects of the lead in fiber for example.

Acknowledgements

The development of the rail-strain-pad was supported by the Austrian Funding Agency (FFG) in cooperation with Getzner Werkstoffe GmbH (DI P. Burtscher, DI M. Dietrich).

References

[1] Auer F (2005) Optimierter Zwischenlagenwechsel bei den ÖBB. ZEVrail Glasers Analen 129: 440-443

[2] Micron Optics (2003) Environmental Simulation & Electrical Testing Report of Compliance for the si425 Swept Laser Interrogator. Technical Manual, Micron Optic, Atlanta, 129 p.

[3] Micron Optics (2004) si425 Optical Sensing Interrogator Instruction Manual. Micron Optics, Atlanta, 79 p.

[4] Micron Optics (2006) Optical Sensing Interrogator si425, Product data sheet No. si425-050321, Micron Optics, http://www.micronoptics.com, 14.09.2006

[5] Moser F (2011) Systemuntersuchungen der FBG Interrogation Unit si425 von Micron Optics. Unpublished Master Thesis, Institute of Engineering Geodesy and Measurement Systems, Graz University of Technology, 154 p.

[6] Woschitz H (2010) Entwicklung eines Rail Strain Pads unter Verwendung von Faser-Bragg-Gitter-Sensoren. In Wunderlich T (ed.) Beiträge zum 16. Internationalen Ingenieurvermessungskurs München 2010. Wichmann: 171-182

[7] Woschitz H (2011) Development of a rail-strain-pad using FBG sensors. 5th Int. Conf. on Structural Health Monitoring of Intelligent Infrastructure (SHMII-5) 2011, 11-15 December 2011, Cancún, México, CD-Proc., 9 p.